JOURNAL OF Materials CHEMISTRY

Supramolecular assembly of a quasi-linear heterofullerene–porphyrin dyad

Frank Hauke,[a] Angela Swartz,[b] Dirk M. Guldi*[b] and Andreas Hirsch*[a]

[a]*Institut für Organische Chemie, Henkestrasse 42, D-91054 Erlangen, Germany. E-mail: hirsch@organik.uni-erlangen.de; Fax: +49 9131 85 26864; Tel: +49 9131 85 22537*
[b]*Radiation Laboratory, University of Notre Dame, IN 46556, USA. E-mail: guldi.1@nd.edu; Fax: +1 219 631 8068; Tel: +1 219 631 7441*

Received 27th February 2002, Accepted 16th April 2002
First published as an Advance Article on the web 14th May 2002

A novel supramolecular dyad (Zn-ttbpp–pyridine–$C_{59}N$)—with a quasi-linear geometry—involving a heterofullerene acceptor and a zinc tetrakis(*p-tert*-butylphenyl)porphyrin (Zn-ttbpp) donor was assembled *via* axial coordination. Depending on the solvent either photoinduced singlet–singlet energy transfer or electron transfer was observed. The latter process takes place in *o*-dichlorobenzene as solvent and leads to the corresponding charge-separated state, that is, the π-radical anion of $C_{59}N$ and the π-radical cation of Zn-ttbpp.

Introduction

The evolution of chemical reactions in nature led to their unprecedented optimization during a time span of millions of years. Therefore, photosynthesis advanced as a highly efficient process, which is used by a wide range of living organisms. The initial step of photosynthesis involves the transduction of the energy of absorbed light from the light-harvesting antenna to the photochemical reaction center. Essential to the function of the reaction center is a relay of short-range charge-separation reactions, evolving among chlorophyll and quinone moieties embedded in a transmembrane protein matrix. Ultimately the product of these cascades is the transformation of light into usable chemical energy.[1] The desire to mimic these complex and highly versatile processes has prompted the design of synthetic ensembles, in which the use of covalent bonds permits the hierarchical integration of multiple components.[2]

The major challenge in these model systems is to generate an energetic, long-lived, charge-separated state in high yields. Formation of the latter depends primarily on a series of factors including nature of the donor–acceptor complex, electronic coupling matrix element, mutual orientation, distance and, finally, solvation dynamics. In this light the synthesis of numerous porphyrin dyads emerged, in which the porphyrin building block functions as the chromophore/electron donor and the acceptor unit is represented by two-dimensional molecules like quinones.

Using C_{60} as an acceptor component bears several advantages in comparison to the quinone-based systems. C_{60}, for example, is a good electron acceptor,[3] which can be reversibly reduced with up to six electrons. More importantly, the rigid three-dimensional framework of fullerenes leads to exceptionally small reorganization energies in charge transfer reactions.[4] And last, but not least, C_{60} exhibits due to its spherical shape a unique platform for supramolecular chemistry.[5–10]

Taking all this into account, it is not surprising that many C_{60}–porphyrin dyads have been synthesized, which give rise to efficient charge-separation events after irradiating the porphyrin moiety with visible light.[11] Such dyads, exemplified by **1**,[12] can be easily built-up *via* the reaction of C_{60} with a porphyrin precursor bearing a malonate group in the presence of CBr_4 and DBU. In this so-called Bingel reaction, cyclopropanation of a [6,6]-double bond of the fullerene framework takes place.[13] Repeating this operation leads to a fullerene bisadduct with two malonic ester functions. The second addition to a [6,6]-double bond imposes, however, the challenge of controlling the regiochemistry.[14] Despite this inherent complication, the bis-addition affords porphyrin bridged C_{60} donor–acceptor dyads like **2**, where the two malonate groups are bound to C_{60} in *trans*-2[14] positions.[15]

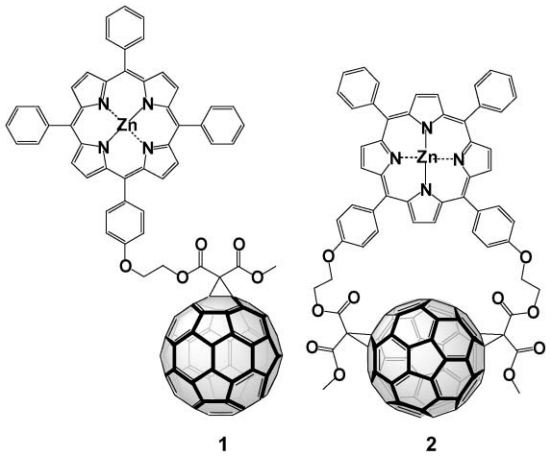

The short van der Waals separation (*edge-to-edge* separation (R_{ee}) ≈ 3.0 Å) in this rather rigid dyad ensures that an *intra*-molecular charge-separation from the porphyrin to the fullerene core succeeds in virtually any solvent.[16–18] Similarly, Diederich *et al.* reported a dyad involving a *trans*-1 addition pattern, which also gives rise to photoinduced electron transfer events.[19]

Charge-separation in C_{60}-based dyads is fine-tuned by varying the donor–acceptor distance or by increasing the donor strength of the porphyrin system.[18] On the other hand, enhancing the acceptor features of the fullerene moiety can be attained by exchanging the parent C_{60} fullerene with, for example, a $C_{59}N$ moiety. Since in $C_{59}N$ one carbon atom of the C_{60} framework is substituted by a nitrogen, an open shell system is created and the simplest derivative constitutes dimer **3**.[20,21] Some of us reported recently on the efficient synthesis of monomeric analogs.[22,23] In the resulting derivatives, which all exhibited better solubility compared to the parent dimer **3**, the $C_{59}N$ moiety is either directly attached to an electron rich aromatic moiety or located α to a carbonyl group. Importantly, all $C_{59}N$ derivatives are better electron acceptors than C_{60} and

 DOI: 10.1039/b202060b

its derivatives.[21] This led us to pursue the attachment of a $C_{59}N$ core to a porphyrin unit, in order to optimize electron transfer kinetics and efficiencies.

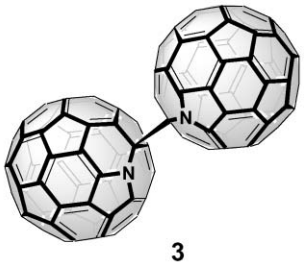

3

The direct cyclopropanation of a porphyrin system bearing a malonate function with a monomeric $C_{59}N$ derivative would be an impractical task. Due to the C_S symmetry of the starting heterofullerene, the second addition can in principle lead to up to 13 C_1 symmetric bisadducts and to only three products with C_S symmetry. A chromatographic separation of the reaction mixture and a subsequent characterization of the addition products would be extremely difficult.

Therefore we devised a supramolecular concept towards the realization of a Zn-ttbpp–pyridine–$C_{59}N$ dyad. Several groups demonstrated the complexation of a zinc tetraphenyl porphyrin with a pyridine derivative carrying a C_{60} core, ZnP–pyridine–C_{60}, with complexation constants ranging from 6000 M^{-1} to 10 000 M^{-1}.[6,24] As far as the solid state structure of ZnP–pyridine–C_{60} is concerned the X-ray structure supports several key features. Firstly, the tilting of the C_{60} unit towards the porphyrin is clearly discernible. Secondly, the edge-to-edge distance, that is, the closest distance between the porphyrin π-ring carbon and the C_{60} carbon of the axially linked fulleroenopyrrolidine is 3.51 Å. Thirdly, the center-to-center distance between the porphyrin zinc ion and C_{60} is ~9.53 Å.

In this article we report a formally unlinked but still well-associated and well-organized porphyrin assembly containing a heterofullerene electron acceptor. Hereby, the use of intermolecular interactions leads to a quasi-linear donor–acceptor ensemble, Zn-ttbpp–pyridine–$C_{59}N$ (**6**), in which the pyridine function holds Zn-ttbpp (**5**) and $C_{59}N$ (**4**) together through reversible, non-covalent—metal-mediated—interactions (Scheme 2).

Results and discussion

Synthesis

Our approach implies the attachment of a donor pyridine ring to the $C_{59}N$ moiety *via* Mannich functionalization of the dimer, which we have established as a versatile tool for the functionalization of azaheterofullerenes.[23] For this purpose 1-(4-pyridyl)ethanone was reacted under standard conditions (*i.e.*, *o*-dichlorobenzene (ODCB) as solvent, 150 °C, *p*-TsOH, air) with $(C_{59}N)_2$ leading to an anchor system, which is expected to coordinate with porphyrin systems (Scheme 1).[25]

After quenching the corresponding conjugated acid with NEt_3 and chromatographic work up on silica gel we obtained **4** in 78% yield. The heterofullerene anchor system **4** was characterized by ^{1}H NMR, ^{13}C NMR, MS and IR spectroscopy.

The ^{13}C NMR spectrum (Fig. 1) confirms the C_S symmetry of the compound. In particular, the fullerene region (δ = 125–156) reveals 28 signals with double and two signals with single intensity. Among the pyridine C-atoms only those at δ = 151.15 and 120.78 were identified, which are located in positions α and β to the nitrogen atom. Conversely, the quaternary C-atom of the pyridine moiety is covered by the signals stemming from the sp^2 C-atoms of the fullerene core. The carbonyl group resonates at δ = 194.13 and the methylene

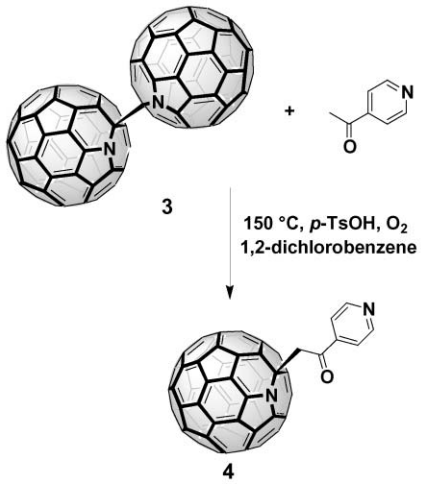

Scheme 1 Synthesis of 2-(azafullerenyl)-1-(4-pyridyl)ethanone **4**.

group at δ = 49.86. Characteristic for all heterofullerene derivatives is the sp^3 carbon atom, which is directly attached to the core N-atom. The signal of this atom is found at δ = 78.27.

In the ^{1}H NMR spectrum the C-atom of the methylene group resonates as a singlet at δ = 5.46. This chemical shift is typical for a C-atom that is located between a carbonyl group and the $C_{59}N$ core.[23] The protons of the pyridine ring give rise to an AA′BB′ spin system. On the other hand, the two protons that are located α to the N-atom form a doublet at δ = 9.04. The signal of the β protons appears at δ = 8.20 as a doublet as well.

^{1}H NMR spectroscopy was employed to confirm the formation of the target complex, that is, Zn-ttbpp–$C_{59}N$ dyad **6**. We therefore dissolved an equimolar amount of the heterofullerene anchor **4** and tetrakis(*p-tert*-butylphenyl)porphyrin (Zn-ttbpp) **5** in deuterated ODCB (Scheme 2) and measured the ^{1}H NMR spectrum *in situ* (see Fig. 2). Besides the new signals of the *ortho* and *meta* protons of the 4 *para*-substituted phenyl rings and the β-pyrrole protons, a fundamental shift of

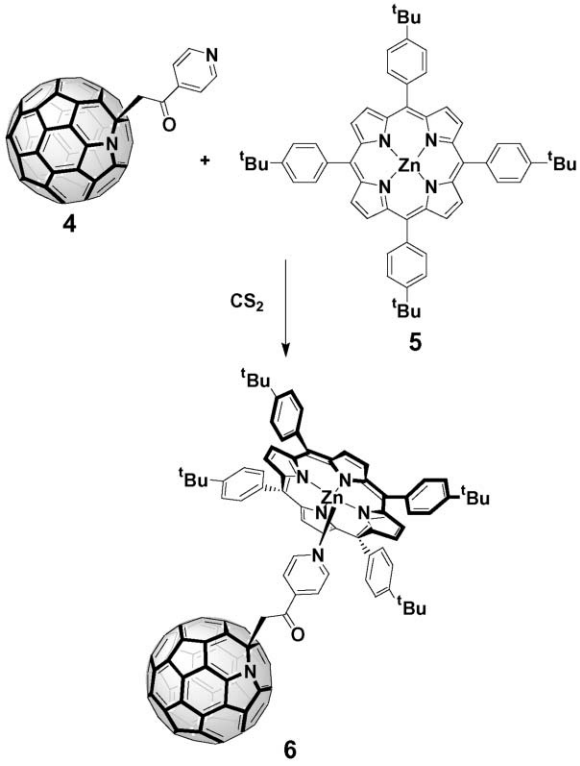

Scheme 2 Synthesis of the macromolecular donor acceptor dyad.

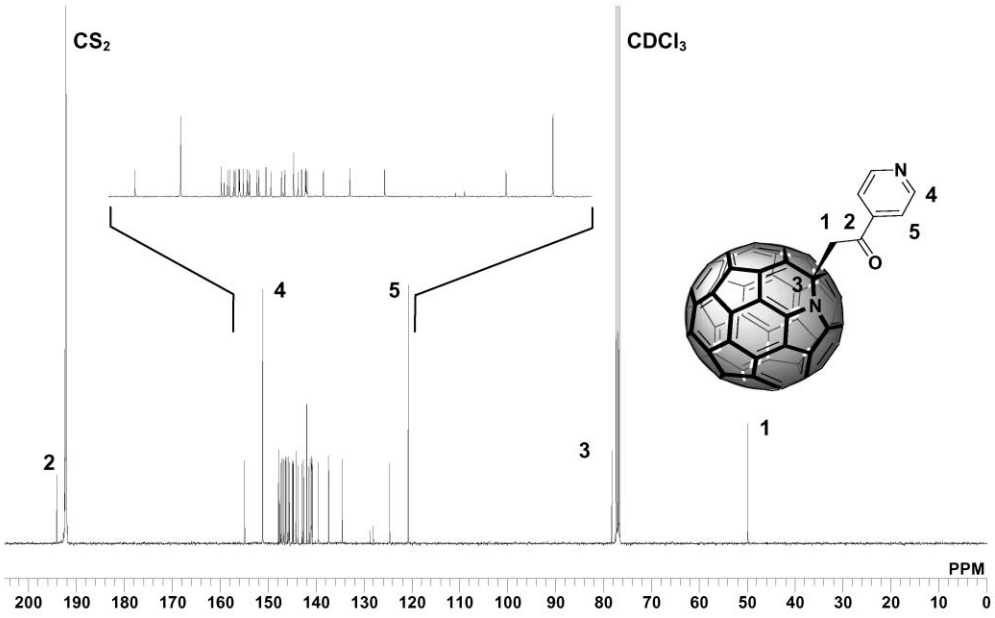

Fig. 1 ^{13}C NMR Spectrum of 2-(azafullerenyl)-1-(4-pyridyl)ethanone (**4**).

the pyridine protons is observed. The signal of the α-pyridine protons is shifted upfield by 4.97 ppm, while the β protons of the pyridine ring are shifted by 1.66 ppm. Even the methylene group is shifted upfield by 0.82 ppm. Importantly, in the ^{1}H NMR spectrum of the equimolar mixture no evidence was seen, which may be associated with the uncomplexed anchor **4**.

In parallel attempts to probe the formation of Zn-ttbpp–C_{59}N (**6**) by absorption spectroscopy, the absorption spectrum of Zn-ttbpp (**5**) was taken at different concentrations of **4**. In toluene solutions the two *Q*-band transitions at 549 nm and 589 nm show, upon adding variable amounts of the fullerene ligand, a noticeable red-shift to 552 nm and 593 nm, respectively. Also the Soret-band is impacted, giving rise to a shift from 423 to 425 nm. Due to the significant absorption of compound **4** in the *Q*-band region, determination of the complex association failed.

Photophysics

The strong emission of metalloporphyrins, with fluorescence quantum yields (Φ) close to unity, renders these chromophores convenient fluorescing markers, especially for the detection of electron and/or energy transfer reactions. We envisaged that metal mediated attractions—stemming from the complexation of pyridine–C_{59}N (**4**) with Zn-ttbpp (**5**)—would induce a supramolecular assembly upon simple mixing of the two components. In fact, adding variable concentrations of **4** (3.5–12 × 10^{-5} M) to a solution of **5** (4.9 × 10^{-5} M) in strictly

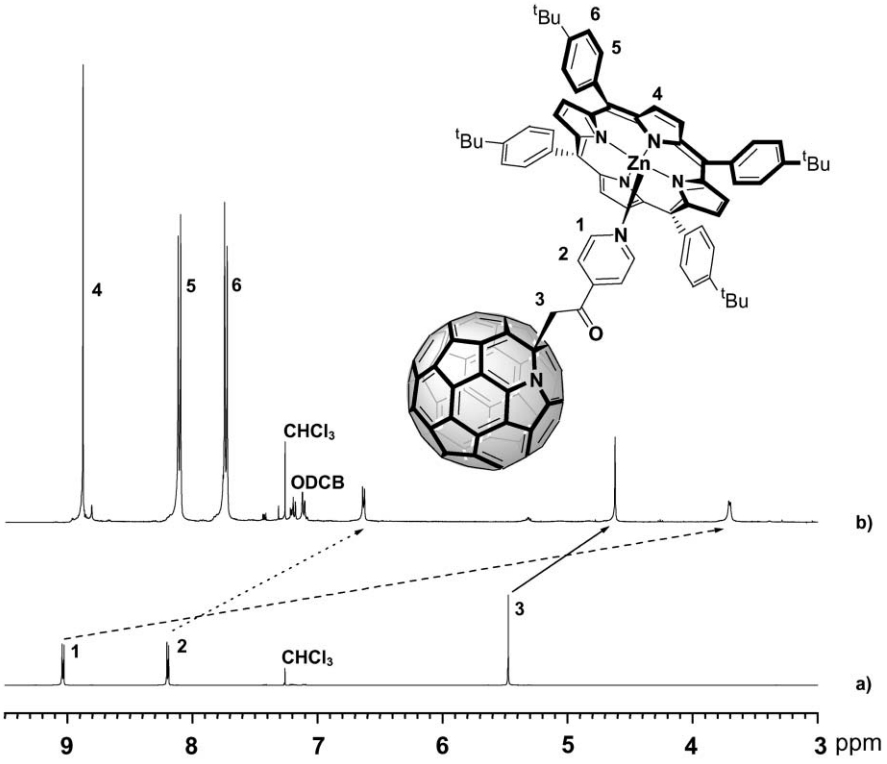

Fig. 2 ^{1}H NMR spectrum of a) 2-(azafullerenyl)-1-(4-pyridyl)ethanone **4** and b) of the porphyrin heterofullerene dyad **6**.

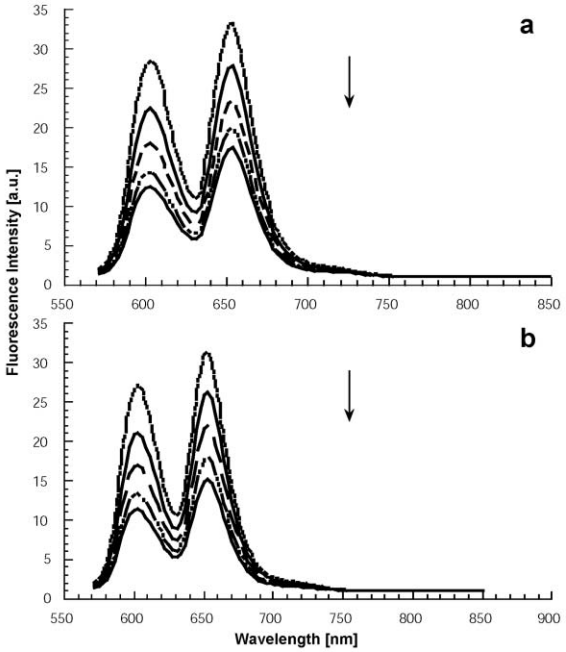

Fig. 3 Fluorescence spectra (λ_{exc} = 545 nm) of Zn-ttbpp (**5**) (3.9 × 10^{-5} M) and variable concentration of heterofullerene anchor **4** (3.5–7.7 × 10^{-5} M) in toluene (a) and *o*-dichlorobenzene (b) at room temperature. Arrows indicate the decreased fluorescence quantum yields with increasing concentration of **4**.

non-coordinating solvents (*i.e.*, toluene or *o*-dichlorobenzene) evoked an incremental quenching of the strong Zn-ttbpp emission (Φ = 0.04). Fig. 3 depicts representative progressions of the fluorescence quenching in toluene and *o*-dichlorobenzene upon exciting into the porphyrin's *Q*-band at 545 nm. A closer inspection of the fluorescence spectra reveals that no influence was seen on the shape and maximum of the spectra.[26]

From complementary time-resolved fluorescence measurements the following trend was derived: Prior to the addition of **4**, the fluorescent signal of **5** is well fitted by a mono-exponential decay, for which a relatively long lifetime of 2.0 ns was determined in deoxygenated toluene. Upon addition of **4**, a double-exponential fluorescence decay is observed with lifetimes of 0.15 ns and 1.9 ns—as shown in Fig. 4. Throughout the titration assay, the two lifetimes are maintained with an increasing contribution of the short-lived component as the concentration of **4** is increased. Essentially, the same picture was gathered in *o*-dichlorobenzene, with the exception that the lifetime of the short-lived component is 0.12 ns. Addition of pyridine or THF restores the original fluorescence intensity, concomitant with the disappearance of the short-lived component, demonstrating that the complex formation is reversible.

In summary, the fluorescence quenching of **5** upon addition of **4** and evidence for a short-lived component, whose intensity increases—but whose lifetime is invariant throughout the titration assay—all are consistent with a static quenching event occurring inside Zn-ttbpp–$C_{59}N$ (**6**). In fact, determining the Zn-ttbpp fluorescence deactivation in **6** by relating the quantum yield (Φ = 0.003) to the quantum yield/lifetime in Zn-ttbpp reference 5, gave a value comparable to the short-lived fluorescence component (0.15 ns). The steady-state fluorescence data were treated by correlating I/I_0 *versus* quencher concentration, using a previously developed procedure to determine the association constant, K_a.[27] In toluene we determined a constant of 9500 ± 300 M^{-1}, while in *o*-dichlorobenzene a slightly larger number, 11 700 ± 700 M^{-1}, was derived.

In toluene, inspection of the 810–840 nm region helped to identify the species evolving from the Zn-ttbpp's singlet excited state quenching in Zn-ttbpp–$C_{59}N$ and, furthermore, to probe the underlying mechanism. In particular, a fluorescence pattern, resembling that of a heterofullerene (*i.e.*, maximum at 825 nm—Fig. 5), such as pyridine–$C_{59}N$ (**4**), was produced, despite the near exclusive excitation of Zn-ttbpp at 545 nm (≫ 90%), in a region where the porphyrin contribution is nearly extinct. The fact that we realize increasing yields of the heterofullerene fluorescence (*i.e.*, $\Phi \approx 1.0 \times 10^{-4}$) throughout the titration experiments, while that of Zn-ttbpp decreases simultaneously, lets us conclude that the heterofullerene singlet excited state is populated.[28] Evidence that this newly formed state is the product of an energy transfer reaction was lent from a set of decisive excitation spectra of the 825 nm fingerprint. The complementary excitation spectrum of the heterofullerene emission in **6** reflects nearly exactly *(i)* the ground-state absorption of Zn-ttbpp and *(ii)* the excitation spectra of Zn-ttbpp with maximum at 430 nm and 545 nm (not shown). Taking all the above evidence into account we reach the conclusion that the origin of the excited state energy is unquestionably that of Zn-ttbpp. It is import to note that the decay of the heterofullerene fluorescence, as measured at 825 nm, is not affected. The lifetime of 1.0 ns is essentially identical to that registered for **4**.

The dynamic character of the weak pyridine–zinc complexation leads to complexation constants of around 10 000 M^{-1}. This refers in large to a weak σ-bonding between the vacant d^{z^2}-orbitals of the zinc metal center and the lone pair of the pyridine's nitrogen. In an attempt to control this labile bonding a separate emission run was conducted in a frozen solvent matrix. Lowering, for example, a room temperature solution of toluene (c_4 = 9.1 × 10^{-5} M) with a statistical distribution of associated Zn-ttbpp–pyridine–$C_{59}N$ and dissociated Zn-ttbpp/pyridine–$C_{59}N$ complexes, to 77 K resulted in a strong

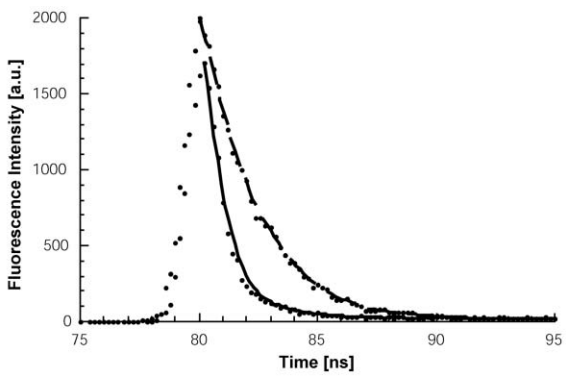

Fig. 4 Time-resolved fluorescence decay of a mixture of Zn-ttbpp (**5**) (3.9 × 10^{-5} M) and heterofullerene anchor **4** (7.7 × 10^{-5} M) as monitored in toluene at the 600 nm emission maximum (dashed line) and internal reference (solid line). Laser excitation was at 337 nm.

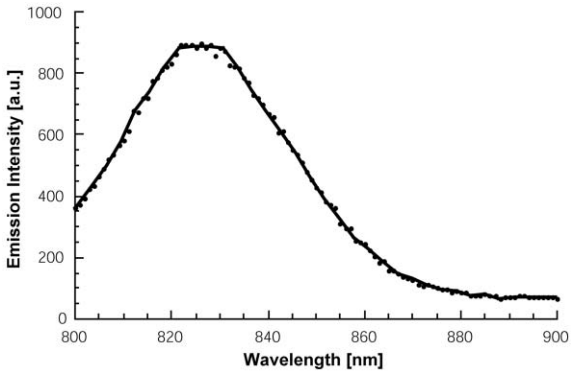

Fig. 5 Fluorescence spectra (λ_{exc} = 545 nm) of a mixture of Zn-ttbpp (**5**) (3.9 × 10^{-5} M) and heterofullerene anchor **4** (7.7 × 10^{-5} M) in toluene at room temperature.

deactivation of the Zn-ttbpp emission from about 47% to nearly 12%. This clearly corroborates the successful freezing of the equilibrium between association (Zn-ttbpp–pyridine–$C_{59}N$) and dissociation (Zn-ttbpp/pyridine–$C_{59}N$).

One of two potential products of the Zn-ttbpp fluorescence quenching ($E_{singlet}$ = 2.02 eV) is the energetically lower lying heterofullerene singlet excited state ($E_{singlet}$ = 1.5 eV),[29] following a transduction of singlet excited state energy. For this pathway we estimate free energy changes ($-\Delta G_{energy\ transfer}$) of 0.52 eV. Alternatively, the charge-separated radical pair, evolving from the Zn-ttbpp singlet excited state to the electron accepting heterofullerene, may be formed. In spite of the lower reduction potential found generally for azafullerenes ($E_{1/2}$ (**4**) = −1140 mV *versus* Fc/Fc^+ in *o*-dichlorobenzene),[30] an intramolecular charge-separation in toluene would be slightly exothermic $-\Delta G_{CS}$ (0.09 eV). Evidently, the much larger energy gap for the energy transfer route evokes a deactivation that is exclusively controlled by energy transfer.

At this point a comparison with the previously reported ZnP–pyridine–C_{60},[24] in which even in toluene charge-separation prevails, is deemed important. The outcome for **6**, namely, a singlet–singlet energy transfer, is rationalized in terms of the spatial distance, separating the Zn-ttbpp donor from the heterofullerene/fullerene acceptor. In particular, the *center-to-center* separation in **6** of 12.68 Å is considerably larger than the separation in the C_{60}-based dyad (9.53 Å). In addition, the substantial tilting of the C_{60} moiety, forces an *edge-to-edge* separation (*i.e.*, the closest distance between the porphyrin π-ring carbon and the C_{60} carbon) of only 3.5 Å. Since the quasi-linear geometry in **6** avoids this puckering, the corresponding *edge-to-edge* separation amounts to 7.1 Å.

Only a substantial increase of the solvent polarity from toluene (ε = 2.38) to *o*-dichlorobenzene (ε = 9.98) brings about the large exothermic driving force for the charge-separation pathway: For example, in *o*-dichlorobenzene, the $-\Delta G_{CS}$ value (0.74 eV) is substantially larger than $-\Delta G_{energy\ transfer}$ (0.52 eV). In line with this energetic presumption, we could not detect in *o*-dichlorobenzene any appreciable heterofullerene emission in the steady-state or time-resolved measurements. This points, indeed, to an alternative deactivation of the Zn-ttbpp singlet excited state, namely, an intramolecular electron transfer (*vide infra*).[31]

To correlate this interesting phenomenon we examined the porphyrin deactivation in Zn-ttbpp–pyridine–$C_{59}N$ (**6**) in relation to Zn-ttbpp (**5**) in a set of complementary experiments. Particularly, the absorption characteristics were monitored following either a short (18 ps) or long (8 ns) 532 nm laser pulse. With the assistance of these experiments we were able to probe the initially excited chromophore, its deactivation and the product identification.

The differential absorption characteristics of zinc porphyrins are well explored. In short, photoexcitation of Zn-ttbpp (**5**) with a 18 ps laser pulse results in characteristic absorption changes, especially in the 500 through 810 nm range. A broad absorption between 570 and 750 nm and a minimum at 550 nm (not shown) mark this new transient. Here, the minima are excellent reflections of the ground state maxima, suggesting the consumption of the Zn-ttbpp ground state as a consequence of converting the porphyrin singlet ground state to the corresponding singlet excited state. Thus, these spectral attributes are indicative of the Zn-ttbpp singlet excited state ($E_{Singlet}$ = 2.02 eV). Importantly, in the near-infrared region (*i.e.*, >750 nm) the singlet excited state absorbs, very weakly as shown in Fig. 6 (*i.e.*, 25 ps time delay). The predominant fate of the transient absorption changes associated with the singlet excited state is intersystem crossing (ISC) to the triplet manifold ($E_{Triplet}$ = 1.53 eV). In the case of **5**, the underlying ISC-kinetics (4.0×10^8 s^{-1}) were determined, from the decay and simultaneous grow-in of the singlet–singlet and triplet–triplet absorption, respectively. The accordingly formed triplet excited state

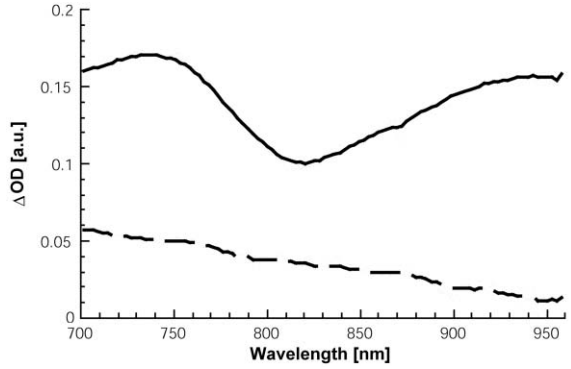

Fig. 6 Picosecond transient absorption spectrum (visible–near-infrared part) recorded 25 ps (dashed line) and 100 ps (solid line) upon flash photolysis of a mixture of Zn-ttbpp (**5**) (3.9×10^{-5} M) and heterofullerene anchor **4** (7.7×10^{-5} M) at 532 nm in deoxygenated toluene.

reveals a characteristic peak around 850 nm (see Fig. 7) and a lifetime of 44 μs.

Upon titration of a toluene solution of **5** (4.9×10^{-5} M) with **4** and excitation at the 535 nm, the lifetime of the Zn-ttbpp singlet excited state transition, although discernible immediately after the short laser pulse, is markedly reduced relative to that in the absence of **4** (2.3 ns). For instance, samples that showed a 79% ($c_{\mathbf{4}} = 3.5 \times 10^{-5}$ M) and a 61% quenching ($c_{\mathbf{4}} = 6.3 \times 10^{-5}$ M) of the fluorescence give rise to lifetimes of 1.8 and 1.5 ns, respectively. Parallel with the faster decay, the Zn-ttbpp singlet excited state features (*i.e.*, Fig. 6; 25 ps time delay) transform, upon addition of **4**, into a new set of transitions with near-infrared maxima at 735 and 940 nm, distinctly different from the Zn-ttbpp triplet excited state transition (*i.e.*, Fig. 6, 100 ps time delay). Insight into the nature of this new transient was lent from a control experiment with **4**. In fact, the differential absorption changes seen for the Zn-ttbpp–pyridine–$C_{59}N$ dyad (**6**) are an exact match to those found immediately upon excitation of the heterofullerene reference (**4**). Again, this further corroborates our assumption that in toluene a rapid singlet–singlet energy transfer governs the fate of the photoexcited porphyrin.[32]

Following the initial transfer of singlet excited state, an intersystem crossing governs the stability of the heterofullerene singlet excited state, for which we determined at the singlet maxima (*i.e.*, 735 and 940 nm) a decay rate of 1.0×10^9 s^{-1}. Later, on the nanosecond, the energetically low-lying heterofullerene triplet excited state, which is formed quantitatively, decays with a lifetime of 15 μs to the singlet ground state. Fig. 7

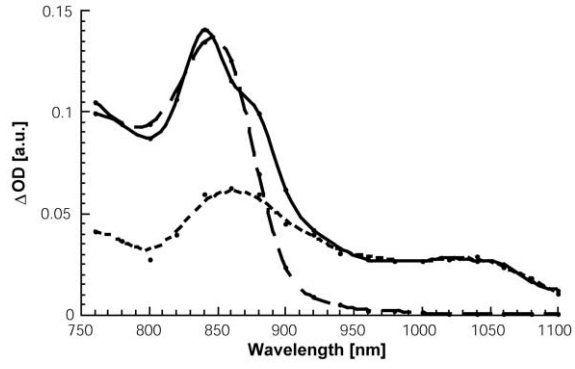

Fig. 7 Nanosecond transient absorption spectrum (visible–near-infrared part) recorded 100 ns upon flash photolysis of Zn-ttbpp (**5**) (3.9×10^{-5} M) (dashed line), heterofullerene anchor **4** (7.7×10^{-5} M) (dotted line) and of a mixture of Zn-ttbpp (**5**) (3.9×10^{-5} M)–heterofullerene anchor **4** (7.7×10^{-5} M) (solid line) at 532 nm in deoxygenated toluene.

summarizes the transient spectra obtained for **4**, **5** and **6**. Again, both decay dynamics—singlet and triplet lifetime—are in good accord with values determined for various heterofullerene references.[28]

In *o*-dichlorobenzene the picture is somewhat different. Following the 18 ps laser pulse of Zn-ttbpp–pyridine–$C_{59}N$ (**6**) ($c_{\text{Zn-ttbpp}} = 4.9 \times 10^{-5}$ M; $c_{\mathbf{4}} = 6.3 \times 10^{-5}$ M), differential absorption changes disclose the instantaneous formation of the Zn-ttbpp singlet excited state. The minimum observed at 555 nm corresponds well to the slightly shifted *Q*-band absorption, due to the complexation of **4**. The singlet lifetime is, however, impacted by the presence of the coordinatively attached electron acceptor. Formation of a new transient develops as a result of the rapid decay, instead of the much slower intersystem crossing (4.0×10^{8} s^{-1}). The new transient absorbs predominantly in a region red-shifted relative to the porphyrin *Q*-bands—similar to Fig. 8. This suggests involvement of the Zn-ttbpp π-radical cation in an intramolecular charge-separation, occurring between the photoexcited Zn-ttbpp donor and the heterofullerene acceptor. With the assistance of complementary nanosecond experiments the presence of the one-electron reduced fullerene, exhibiting a characteristic absorption maximum at 1020 nm,[28] was also confirmed. The charge-separated radical pair, $(\text{Zn-ttbpp})^{+}$–pyridine–$(C_{59}N)^{-}$, is metastable and decays with a rate constant of 6.9×10^{6} s^{-1}.

To probe a coordinating solvent, which may potentially interfere with the association of the two chromophores (Zn-ttbpp–pyridine–$C_{59}N$), similar concentrations of **4** and **5** were combined in benzonitrile. Hereby, the Zn-ttbpp fluorescence is just marginally affected (up to 5%, not shown) relative to the dramatic changes seen in the cases of toluene and *o*-dichlorobenzene (~50%). At this point we would like to emphasize that the absence of an efficient deactivation does not necessarily implement the free energy changes associated with intramolecular events, since they are sufficiently exothermic. Instead, the formation of a Zn-ttbpp–benzonitrile complex limits the reaction between the photoexcited electron donor and the electron accepting $C_{59}N$ moiety to an intermolecular process yielding the dissociated and free radical ions, that is, the heterofullerene π-radical anion ($\lambda_{\max} = 1020$ nm) and the Zn-ttbpp π-radical cation ($\lambda_{\max} = 640$ nm). To illustrate this, in Fig. 8 the transient absorption spectrum recorded 100 ns after the 532 nm laser pulse and are compared with that seen at 10 μs. The actual charge-separation rate was derived from a concentration dependent decay of the Zn-ttbpp triplet excited state and further confirmed by the simultaneous grow-in of the radical ions: Overall a nearly diffusion-controlled rate constant of 1.5×10^{9} $M^{-1}s^{-1}$ was found.

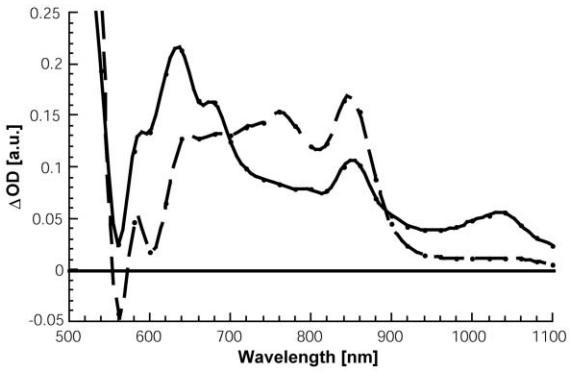

Fig. 8 Nanosecond transient absorption spectrum (visible–near-infrared part) recorded 100 ns (dashed line) and 10 μs (solid line) upon flash photolysis of a mixture of Zn-ttbpp (**5**) (3.9×10^{-5} M) and heterofullerene anchor **4** (7.7×10^{-5} M) at 535 nm in deoxygenated benzonitrile.

Conclusion

We have demonstrated that supramolecular architectures based on a heterofullerene and a zinc porphyrin are readily formed by the complexation of a pyridine moiety covalently bound to the heterofullerene with the central zinc atom of the porphyrin. This adduct is ideally suited for devising integrated model systems to transmit and process solar energy.

Experimental

General remarks and materials

Picosecond laser flash photolysis experiments were carried out with 532 nm laser pulses from a mode-locked, Q-switched Quantel YG-501 DP ND : YAG laser system (pulse width ≈ 18 ps, 2–3 mJ per pulse). Nanosecond Laser Flash Photolysis experiments were performed with laser pulses from a Quanta-Ray CDR Nd: YAG system (532 nm, 6 ns pulse width) in a front face excitation geometry. Emission spectra were recorded with a SLM 8100 Spectrofluorometer. The experiments were performed at room temperature. A 570 nm long-pass filter in the emission path was used in order to eliminate the interference from the solvent and stray light for recording the fullerene fluorescence. Each spectrum was an average of at least 5 individual scans and the appropriate corrections were applied.

$(C_{59}N)_2$ was prepared according to a literature procedure.[33] ^{1}H and ^{13}C NMR spectra were obtained from JEOL JNM EX and JEOL JNM GX instruments. Mass spectral data were obtained on a Varian MAT 311 A mass spectrometer. UV–VIS spectra were recorded on a Shimadzu UV-3102 spectrometer. IR spectra were obtained on a Bruker Vektor 22 instrument. HPLC analyses have been carried out on a Cosmosil Buckyprep Waters column (250 × 4.6 mm) using toluene as eluent.

Synthesis of 4 and spectroscopic data of 4 and 6

The heterofullerene dimer **3** (30 mg (20.83 μmol)) and 2 g (300 eq.) *p*-TsOH were dissolved in 100 mL ODCB. In a dropping funnel 850 mg (200 eq.) 1-(4-pyridyl)ethanone was dissolved in 20 mL of ODCB. The hetrofullerene solution was heated to 150 °C while passing a constant stream of air through the solution. The pyridine derivative was slowly added to the reaction mixture. The reaction was monitored by TLC (silica gel, toluene–ethyl acetate 9 : 1). After about 30 min the reaction mixture was cooled down and 2 mL NEt_3 were added to neutralize the acid. The product was isolated by flash chromatography using toluene as eluent. For further purification **4** was precipitated from CS_2–pentane, washed three times with pentane and dried in high vacuum. The yield of **4** was 78%.

ν(KBr)/cm^{-1}: 2925, 2922, 2904, 2872, 1703, 1636, 1584, 1552, 1508, 1459, 1423, 1406, 1352, 1327, 1291, 1219, 1186, 1174, 1092, 1063, 1045, 1000, 806, 790, 768, 745, 721, 669, 644, 578, 556, 524 and 504; $\lambda_{\max}$(ODCB)/nm (ε) 322 (29694), 245 (7394), 596 (3252), 724 (2485); ^{13}C NMR δ (100 MHz, CS_2–$CDCl_3$) 194.13 (C=O, 1C), 154.87, 151.15 (2C, py), 147.84, 147.61 (1C), 147.33, 147.17, 146.85, 146.71, 146.40, 146.34, 146.05, 145.74, 145.62 (1C), 145.53, 144.92, 144.76, 144.20, 144.18, 143.79, 142.92, 142.64, 141.92 (4C), 141.57, 141.27, 140.96, 140.90, 140.81, 139.51, 137.36, 134.50, 124.59, 120.78 (2C, py), 78.27 (1C, sp^3), 49.86 (1C, CH_2); ^{1}H NMR δ (400 MHz, CS_2–$CDCl_3$) 9.04 (AA′XX′, 2H, αH-py), 8.20 (AA′XX′, 2H, βH-py), 5.47 (s, 2H, CH_2); *m*/*z* (EI) 842 (M^{+}), 722 ($C_{59}N$).

NMR spectroscopic data for compound **6**: ^{13}C NMR δ (100 MHz, $CDCl_3$) 192.49 (C=O, 1C), 154.28, 149.80 (porph), 149.29 (porph), 147.25 (1C), 147.08, 146.93, 146.76, 146.41, 146.10, 146.05, 145.97, 145.87, 145.70, 145.37, 145.19, 144.58, 144.38 (1C), 143.83, 143.40, 142.56, 142.30, 141.56, 141.20, 141.18, 140.90, 140.48, 140.46, 139.95 (porph), 139.06, 136.85,

134.27 (porph), 133.96, 131.66 (porph), 128.75, 128.00, 125.11, 124.06, 123.14 (porph), 120.51 (porph), 119.69, 77.57 (1C, sp^3), 49.21 (1C, CH_2), 34.31 (4C, ^{t}Bu), 31.54 (12C, CH_3, ^{t}Bu); ^{1}H NMR δ (400 MHz, $CDCl_3$) 9.21 (s, 8H, βH-porph), 8.46 (''d'', 8H, (CH-ph), 8.00 (''d'', 8H, (CH-ph), 6.54 (br ''d'', 2H, βH-py), 4.65 (s, 2H, CH_2), 4.07 (br s, 2H, αH-py), 1.75 (36 H, CH_3 ^{t}Bu).

Acknowledgement

This work was supported by the Deutsche Forschungsgemeinschaft (DFG) and the Office of Basic Energy Sciences of the U.S. Department of Energy. This is document NDRL-4380 from the Notre Dame Radiation Laboratory.

References

1 *The Photosynthetic Reaction Center*, ed. J. Deisenhofer and J.R. Norris, Academic Press, New York, 1993.
2 (*a*) M.-J. Blanco, M. C. Jimenez, J. C. Chambron, V. Heitz, M. Linke and J. P. Sauvage, *Chem. Soc. Rev.*, 1999, **28**, 293; (*b*) M. N. Paddon-Row, *Acc. Chem. Res.*, 1994, **27**, 18; (*c*) M. R. Wasielewski, *Chem. Rev.*, 1992, **92**, 435.
3 L. Echegoyen and L. E. Echegoyen, *Acc. Chem. Res.*, 1998, **31**, 593–601.
4 D. M. Guldi and M. Prato, *Acc. Chem. Res.*, 2000, **33**, 695–703.
5 A. Hirsch, *Chemistry of the Fullerenes*, Thieme, New York, 1994.
6 F. Diederich and M. Gomez-Lopez, *Chem. Soc. Rev.*, 1999, **28**, 263–277.
7 F. Diederich and R. Kessinger, *Acc. Chem. Res.*, 1999, **32**, 537–545.
8 M. Brettreich, S. Burghardt, C. Bottcher, T. Bayerl, S. Bayerl and A. Hirsch, *Angew. Chem., Int. Ed.*, 2000, **39**, 1845–1848.
9 A. Herzog, A. Hirsch and O. Vostrowsky, *Eur. J. Org. Chem.*, **2000**, 171–180.
10 F. Djojo, E. Ravanelli, O. Vostrowsky and A. Hirsch, *Eur. J. Org. Chem.*, 2000, 1051–1059.
11 (*a*) M. Prato, *J. Mater. Chem.*, 1997, **7**, 1097–1109; (*b*) N. Martin, L. Sanchez, B. Illescas and I. Perez, *Chem. Rev.*, 1998, **98**, 2527–2547; (*c*) H. Imahori and Y. Sakata, *Eur. J. Org. Chem.*, 1999, 2445–2457; (*d*) D. M. Guldi, *Chem. Commun.*, 2000, 321–327; (*e*) D. Gust, T. A. Moore and A. L. Moore, *Acc. Chem. Res.*, 2001, **34**, 40–48.
12 E. Dietel, A. Hirsch, J. Zhou and A. Rieker, *J. Chem. Soc., Perkin Trans. 2*, 1998, 1357–1364.
13 C. Bingel, *Chem. Ber.*, 1993, **126**, 1957.
14 A. Hirsch, I. Lamparth and H. R. Karfunkel, *Angew. Chem.*, 1994, **106**, 453–455*Angew. Chem., Int. Ed. Engl.1994,* **33**, 437–438.
15 E. Dietel, A. Hirsch, E. Eichhorn, A. Rieker, S. Hackbarth and B. Roder, *Chem. Commun.*, 1998, 1981–1982.
16 D. M. Guldi, C. Luo, T. Da Ros, M. Prato, E. Dietel and A. Hirsch, *Chem. Commun.*, 2000, 375–376.
17 D. M. Guldi, C. Luo, M. Prato, E. Dietel and A. Hirsch, *Chem. Commun.*, 2000, 373–374.
18 D. M. Guldi, C. Luo, M. Prato, A. Troisi, F. Zerbetto, M. Scheloske, E. Dietel, W. Bauer and A. Hirsch, *J. Am. Chem. Soc.*, 2001, **123**, 9166–9167.
19 J.-P. Bourgeois, F. Diederich, L. Echegoyen and J.-F. Nierengarten, *Helv. Chim. Acta*, 1998, **81**, 1835–1844.
20 C. Bellavia-Lund, M. Keshavarz-K, T. Collins and F. Wudl, *J. Am. Chem. Soc.*, 1997, **119**, 8101–8102.
21 A. Hirsch and B. Nuber, *Acc. Chem. Res.*, 1999, **32**, 795–804.
22 B. Nuber and A. Hirsch, *Chem. Commun.*, 1998, 405–406.
23 (*a*) F. Hauke and A. Hirsch, *Chem. Commun.*, 1999, 2199–2200; (*b*) F. Hauke and A. Hirsch, *Tetrahedron*, 2001, **57**, 3697.
24 (*a*) T. D. Ros, M. Prato, D. M. Guldi, M. Ruzzi and L. Pasimeni, *Chem. Eur. J.*, 2001, **7**, 816–827; (*b*) F. D'Souza, G. R. Deviprasad, M. S. Rahman and J.-P. Choi, *Inorg. Chem.*, 1999, **38**, 2157–2160; (*c*) F. D'Souza, N. P. Rath, G. R. Deviprasad and M. E. Zandler, *Chem. Commun.*, 2001, 267–268; (*d*) N. Armaroli, F. Diederich, L. Echegoyen, T. Habicher, L. Flamigni, G. Marconi and J.-F. Nierengarten, *New. J. Chem.*, 1999, 77–83.
25 Leading examples: (*a*) C. A. Hunter, J. K. M. Sanders, G. S. Beddart and S. Evans, *Chem. Commun.*, 1989, 1765–1766; (*b*) C. A. Hunter and R. K. Hyde, *Angew. Chem., Int. Ed.*, 1996, **35**, 1936; (*c*) C. A. Hunter and R. J. Shannon, *Chem. Commun.*, 1996, 1361–1362.
26 By contrast, addition of suitable fullerene references that lack the presence of the coordination motif, namely, the pyridine functionality, led only to an insignificant regression of the Zn-ttbpp fluorescence that amounts to less than 10% within in the same concentration range.
27 F. Hauke, A. Hirsch, S.-G Liu, L. Echegoyen, A. Swartz, C. Luo and D. M. Guldi, *ChemPhysChem*, 2002, **3**, 195–201.
28 This may, at least, in part be due to a steady increasing contribution of the $C_{59}N$ absorption in ZnP–$C_{59}N$ at the 532 nm excitation wavelength. To rule out this possible but unlikely hypothesis, the emission spectra of several mixtures—**4** plus **5**—in benzonitrile were considered. In benzonitrile the 775–900 nm region lacks the emissive fingerprint of the azafullerene at all, which suggests that the direct contribution is unlikely to prevail even in toluene.
29 L. Famigni and M. B. Johnston, *New. J. Chem.*, 2001, **25**, 1368–1371.
30 The driving forces ($-\Delta G_{CR}^{\circ}$/eV) for the intramolecular charge-recombination (CR) processes were calculated by applying eqn. (1):

$$-\Delta G_{CR}^{\circ} = E_{1/2}(D^{\bullet +}/D) - E_{1/2}(A/A^{\bullet -}) + \Delta G_S \quad (1)$$

where $E^{\circ}_{1/2}(D^{\bullet +}/D)$ is the first one-electron oxidation potential of the Zn-ttbpp donor moiety (+270 mV *versus* Fc/Fc^+ in *o*-dichlorobenzene), while $E^{\circ}_{1/2}(A/A^{\bullet -})$ refers to the first one-electron reduction potential of the $C_{59}N$ electron acceptor (−1140 mV *versus* Fc/Fc^+ in *o*-dichlorobenzene). In the next step we elucidate the role of the solvent (ΔG_S) on the relative energy of the charge-separated state by referring to the ''Dielectric Continuum Model'':

$$\Delta G_S = \frac{e^2}{4\pi\varepsilon_0}\left[\left(\frac{1}{2R_+} + \frac{1}{2R_-} - \frac{1}{R_{D-A}}\right)\frac{1}{\varepsilon_S} - \left(\frac{1}{2R_+} + \frac{1}{2R_-}\right)\frac{1}{\varepsilon_R}\right] \quad (2)$$

Furthermore, the driving forces ($-\Delta G_{CS}^{\circ}$/eV) for the intramolecular charge-separation (CS) processes were determined by:

$$-\Delta G_{CS}^{\circ} = \Delta E_{0-0} - (-\Delta G_{CR}) \quad (3)$$

Hereby, ΔE_{0-0} is the energy of the 0–0 transition energy gap between the lowest excited state and the ground state (2.00 eV).
31 A similar behavior was reported in (*a*) H. Imahori, K. Hagiwara, M. Aoki, T. Akiyama, S. Taniguchi, T. Okada, M. Shirakawa and Y. Sakata, *J. Am. Chem. Soc.*, 1996, **118**, 11771–11782; (*b*) C. Luo, D. M. Guldi, H. Imahori, K. Tamaki and Y. Sakata, *J. Am. Chem. Soc.*, 2000, **122**, 6535–6551.
32 On the picosecond time scale yet another contribution remains evident. The latter agrees well with the unquenched Zn-ttbpp singlet–singlet absorption, which slowly transforms into the corresponding triplet features. Similarly, the differential absorption changes in the nano-/millisecond regimes reveal two contributions, as summarized in Fig. 7. They constitute the features of the porphyrin triplet excited state (λ_{max} = 850 nm), relating to the dissociated, free porphyrin and those of the azafullerene triplet (λ_{max} = 850 and 1040 nm), stemming from the sequence of energy transfer and intersystem crossing in the associated dyad (**6**). Increasing the azafullerene up to 9.1×10^{-5} M did not change this picture, with the exception that the unquenched Zn-ttbpp singlet–singlet transitions weaken progressively with concentration. This reflects the shifting of the equilibrium to the right hand side, that is, the associated Zn-ttbpp–pyridine–$C_{59}N$ (**6**) and, in turn, enhancing the intramolecular contribution relative to the limiting intersystem crossing kinetics of free **5**. Furthermore, it confirms the qualitative picture concluded from the fluorescence experiments.
33 J. C. Hummelen, B. Knight, J. Pavlovich, R. González and F. Wudl, *Science*, 1995, **269**, 1554–1556.